Perspectives and Challenges for QCD Phenomenology*

Stanley J. Brodsky†
Stanford Linear Accelerator Center, 2572 Sand Hill Road, Menlo Park, CA 94025

A fundamental understanding of quantum chromodynamics, particularly at the amplitude level, is essential for progress in high energy physics. For example, the measurement and interpretation of the basic parameters of the electroweak theory and CP violation depends on an understanding of the dynamics and phase structure of exclusive B-meson decay amplitudes. In this review, I discuss a number of ways in which the required hadron wavefunctions can be measured (such as two-photon reactions and diffractive dissociation) or calculated from first principles. An important tool for describing relativistic composite systems in quantum field theory is the light-front Fock expansion, which encodes the properties of a hadrons in terms of a set of frame-independent $n-$particle wavefunctions. Light-front quantization in the doubly-transverse light-cone gauge has a number of remarkable advantages, including explicit unitarity, the absence of ghost degrees of freedom, and the decoupling properties needed to prove factorization theorems in high momentum transfer inclusive and exclusive reactions. Evolution in light-cone time allows the construction of an "event amplitude generator" in which only non-ghost physical degrees of freedom and integration over physical phase appear. The diffractive dissociation of a hadron at high energies, by either Coulomb or Pomeron exchange, has a natural description in QCD as the materialization of the projectile's light-cone wavefunctions; in particular, the diffractive dissociation of a meson, baryon, or photon into high transverse momentum jets measures the shape and other features of the projectile's distribution amplitude. Diffractive dissociation can thus test fundamental properties of QCD, including color transparency and intrinsic charm. I also review recent work which shows that the structure functions measured in deep inelastic lepton scattering are affected by final-state rescattering, thus modifying their connection with the light-cone probability distributions. In particular, the shadowing of nuclear structure functions is due to destructive interference effects from leading-twist diffraction of the virtual photon, physics not included in the nuclear light-cone wavefunctions.

1. Introduction

Quantum chromodynamics is the bedrock of the Standard Model, providing a fundamental description of hadron physics in terms of quark and gluon degrees of freedom. The theory has been tested extensively, particularly in inclusive and exclusive processes involving collisions at large momentum transfer where factorization theorems and the smallness of the QCD effective coupling allow perturbative predictions. QCD is an extraordinarily complex and rich theory, leading to many remarkable and novel physical phenomena. However, continued testing and development of QCD, particularly at the amplitude level, is crucial for progress in high energy physics. For example, the measurement and interpretation of the basic parameters of electroweak theory and CP violation depends on an understanding of the dynamics and phase structure of exclusive B-meson decays amplitudes and the contributing hadronic wavefunctions.

Despite its empirical successes, many fundamental questions about QCD have not been resolved. These include a fundamental understanding of hadronization and color confinement, the behavior of the QCD coupling at small momenta, the problem of asymptotic $n!$ growth of the perturbation theory (renormalon phenomena), the nature of diffractive phenomena, a fundamental theory of the soft and hard aspects of the pomeron in high energy reactions, the origin of shadowing and anti-shadowing in nuclear collisions, the apparent conflict between QCD vacuum structure and the small size of the cosmological constant. There are also a number of empirical puzzles, such as the anomalous size of the $b\overline{b}$ production cross section at hadron colliders, the $J/\psi \to \rho\pi$ puzzle, the apparent small size of spin in the proton, the strong spin correlations in large angle proton-proton elastic scattering, the momentum spectrum of J/ψ in B decays, the un-

*Work supported by Department of Energy contract DE–AC03–76SF00515.
†Electronic address: sjbth@slac.stanford.edu

usual pattern of color transparency effects in quasi-elastic reactions, and the anomalous nuclear dependence of nuclear structure functions at small momentum transfer.

2. Light-Front Wavefunctions

One of the important theoretical goals in QCD is a frame-independent, quantum-mechanical representation of hadrons at the amplitude level capable of encoding multi-quark, hidden-color and gluon momentum, helicity, and flavor correlations in the form of universal process-independent hadron wavefunctions. Light-front quantization allows a unified relativistic wavefunction representation of non-perturbative hadron dynamics in QCD. Furthermore, it is possible to measure the wavefunctions of a relativistic hadron by diffractively dissociating it into jets whose momentum distribution is correlated with the valence quarks' momenta [1, 2, 3, 4]. It is particularly important to understand the shape of the gauge- and process-independent meson and baryon valence-quark distribution amplitudes [5] $\phi_M(x,Q)$, and $\phi_B(x_i,Q)$. These quantities specify how a hadron shares its longitudinal momentum among its valence quarks; they control virtually all exclusive processes involving a hard scale Q, including form factors, Compton scattering and photoproduction at large momentum transfer, as well as the decay of a heavy hadron into specific final states [6, 7].

In light-front quantization, one takes the light-cone time variable $t+z/c$ as the evolution parameter instead of ordinary time t. (The $\hat{z}$ direction is an arbitrary reference direction.) The method is often called "light-front" quantization rather than "light-cone" quantization since the equation $x^+ = \tau = 0$ defines a hyperplane corresponding to a light-front. The light-front fixes the initial boundary conditions of a composite system as its constituents are intercepted by a light-wave evaluated at a specific value of $x^+ = t + z/c$. In contrast, determining an atomic wavefunction at a given instant $t = t_0$ requires measuring the simultaneous scattering of Z photons on the Z electrons. An extensive review and guide to the light-front quantization literature can be found in Ref. [8]. I will use here the notation $A^\mu = (A^+, A-, A_\perp)$, where $A^\pm = A^0 \pm A^z$ and the metric $A \cdot B = \frac{1}{2}(A^+B^- + A^-B^+) - A_\perp \cdot B_\perp$.

It is convenient to define the invariant light-front Hamiltonian: $H_{LC}^{QCD} = P^+P^- - \vec{P}_\perp^2$ where $P^\pm = P^0 \pm P^z$. The operator $P^- = i\frac{d}{d\tau}$ generates light-cone time translations. The P^+ and $\vec{P}_\perp$ momentum operators are independent of the interactions, and thus are conserved at all orders. The eigen-spectrum of H_{LC}^{QCD} in principle gives the entire mass squared spectrum of color-singlet hadron states in QCD, together with their respective light-front wavefunctions. For example, the proton state satisfies: $H_{LC}^{QCD}|\Psi_p\rangle = M_p^2|\Psi_p\rangle$. The projection of the proton's eigensolution $|\Psi_p\rangle$ on the color-singlet $B = 1$, $Q = 1$ eigenstates $\{|n\rangle\}$ of the free Hamiltonian $H_{LC}^{QCD}(g = 0)$ gives the light-front Fock expansion: [9]

$$\left|\Psi_p; P^+, \vec{P}_\perp, \lambda\right\rangle = \sum_{n\geq 3,\lambda_i} \int \Pi_{i=1}^n \frac{d^2k_{\perp i}dx_i}{\sqrt{x_i}16\pi^3} 16\pi^3 \delta\left(1 - \sum_j^n x_j\right) \delta^{(2)}\left(\sum_\ell^n \vec{k}_{\perp\ell}\right) \times \left|n; x_iP^+, x_i\vec{P}_\perp + \vec{k}_{\perp i}, \lambda_i\right\rangle \psi_{n/p}(x_i, \vec{k}_{\perp i}, \lambda_i) \ . \tag{1}$$

The light-front Fock wavefunctions $\psi_{n/H}(x_i, \vec{k}_{\perp i}, \lambda_i)$ interpolate between the hadron H and its quark and gluon degrees of freedom. The light-cone momentum fractions of the constituents, $x_i = k_i^+/P^+$ with $\sum_{i=1}^n x_i = 1$, and the transverse momenta $\vec{k}_{\perp i}$ with $\sum_{i=1}^n \vec{k}_{\perp i} = \vec{0}_\perp$ appear as the momentum coordinates of the light-front Fock wavefunctions. A crucial feature is the frame-independence of the light-front wavefunctions. The x_i and $\vec{k}_{\perp i}$ are relative coordinates independent of the hadron's momentum P^μ. The actual physical transverse momenta are $\vec{p}_{\perp i} = x_i\vec{P}_\perp + \vec{k}_{\perp i}$. The λ_i label the light-front spin S^z projections of the quarks and gluons along the z direction. The physical gluon polarization vectors $\varepsilon^\mu(k, \lambda = \pm 1)$ are specified in light-cone gauge by the conditions $k \cdot \varepsilon = 0$, $\eta \cdot \varepsilon = \varepsilon^+ = 0$. Each light-front Fock wavefunction satisfies conservation of the z projection of angular momentum: $J^z = \sum_{i=1}^n S_i^z + \sum_{j=1}^{n-1} l_j^z$. The sum over S_i^z represents the contribution of the intrinsic spins of the n Fock state constituents. The sum over orbital angular momenta $l_j^z = -i(k_j^1 \frac{\partial}{\partial k_j^2} - k_j^2 \frac{\partial}{\partial k_j^1})$ derives from the $n-1$ relative momenta. This excludes the

contribution to the orbital angular momentum due to the motion of the center of mass, which is not an intrinsic property of the hadron [10].

Light-cone wavefunctions represent the ensemble of states possible when the hadron is intercepted by a light-front at fixed $\tau = t + z/c$. The light-cone representation thus provide a frame-independent, quantum-mechanical representation of the incoming hadron at the amplitude level, capable of encoding its multi-quark, hidden-color and gluon momentum, helicity, and flavor correlations in the form of universal process-independent hadron wavefunctions.

It is especially convenient to develop the light-front formalism in the light-cone gauge $A^+ = A^0 + A^z = 0$. In this gauge the A^- field becomes a dependent degree of freedom, and it can be eliminated from the gauge theory Hamiltonian, with the addition of a set of specific instantaneous light-cone time interactions. In fact in $QCD(1+1)$ theory, this instantaneous interaction provides the confining linear x^- interaction between quarks. In $3+1$ dimensions, the transverse field $A^\perp$ propagates massless spin-one gluon quanta with two polarization vectors [5] which satisfy both the gauge condition $\varepsilon^+_\lambda = 0$ and the Lorentz condition $k \cdot \varepsilon = 0$. Thus no extra condition on the Hilbert space is required [11].

There are a number of other simplifications of the light-front formalism:

1. The light-front wavefunctions describe quanta which have positive energy, positive norm, and physical polarization. The formalism is thus physical, and unitary. No ghosts fields appear explicitly, even in non-Abelian theory. The wavefunctions are only functions of three rather than four physical momentum variables: the light-front momentum fractions x_i and transverse momenta $k_\perp$. The quarks and gluons each have two physical polarization states. The Ward identities for vertex and wavefunction renormalization are simple for these physical quanta.

2. The set of light-front wavefunctions provide a frame-independent, quantum-mechanical description of hadrons at the amplitude level capable of encoding multi-quark and gluon momentum, helicity, and flavor correlations in the form of universal process-independent hadron wavefunctions. Matrix elements of spacelike currents such as the spacelike electromagnetic form factors have an exact representation in terms of simple overlaps of the light-front wavefunctions in momentum space with the same x_i and unchanged parton number [12, 13, 14]. In the case of timelike decays, such as those determined by semileptonic B decay, one needs to include contributions in which the parton number $\Delta n = 2$ [15]. The leading-twist off-forward parton distributions measured in deeply virtual Compton scattering have a similar light-front wavefunction representation [16, 17].

3. The high $x \to 1$ and high $k_\perp$ limits of the hadron wavefunctions control processes and reactions in which the hadron wavefunctions are highly stressed. Such configurations involve far-off-shell intermediate states and can be systematically treated in perturbation theory [5, 18].

4. The leading-twist structure functions $q_i(x,Q)$ and $g(x,Q)$ measured in deep inelastic scattering can be computed from the absolute squares of the light-front wavefunctions, integrated over the transverse momentum up to the resolution scale Q. All helicity distributions are thus encoded in terms of the light-front wavefunctions. The DGLAP evolution of the structure functions can be derived from the high $k_\perp$ properties of the light-front wavefunctions. Thus given the light-front wavefunctions, one can compute [5] all of the leading twist helicity and transversity distributions measured in polarized deep inelastic lepton scattering. For example, the helicity-specific quark distributions at resolution Λ correspond to

$$q_{\lambda_q/\Lambda_p}(x,\Lambda) = \sum_{n,q_a} \int \prod_{j=1}^{n} \frac{dx_j d^2k_{\perp j}}{16\pi^3} \sum_{\lambda_i} |\psi^{(\Lambda)}_{n/H}(x_i,\vec{k}_{\perp i},\lambda_i)|^2 \times 16\pi^3 \delta\left(1-\sum_i^n x_i\right) \delta^{(2)}\left(\sum_i^n \vec{k}_{\perp i}\right) \delta(x-x_q)\delta_{\lambda,\lambda_q}\Theta(\Lambda^2-\mathcal{M}_n^2)\ , \tag{2}$$

where the sum is over all quarks q_a which match the quantum numbers, light-front momentum fraction x, and helicity of the struck quark. Similarly, the transversity distributions and

off-diagonal helicity convolutions are defined as a density matrix of the light-front wavefunctions. This defines the LC factorization scheme [5] where the invariant mass squared $\mathcal{M}_n^2 = \sum_{i=1}^{n} (k_{\perp i}^2 + m_i^2)/x_i$ of the n partons of the light-front wavefunctions is limited to $\mathcal{M}_n^2 < \Lambda^2$.

5. The distribution of spectator particles in the final state in the proton fragmentation region in deep inelastic scattering at an electron-proton collider are encoded in the light-front wavefunctions of the target proton. Conversely, the light-front wavefunctions can be used to describe the coalescence of comoving quarks into final state hadrons.

6. The light-front wavefunctions also specify the multi-quark and gluon correlations of the hadron. Despite the many sources of power-law corrections to the deep inelastic cross section, certain types of dynamical contributions will stand out at large x_{bj} since they arise from compact, highly-correlated fluctuations of the proton wavefunction. In particular, there are particularly interesting dynamical $\mathcal{O}(1/Q^2)$ corrections which are due to the *interference* of quark currents; *i.e.*, contributions which involve leptons scattering amplitudes from two different quarks of the target nucleon [19].

7. The higher Fock states of the light hadrons describe the sea quark structure of the deep inelastic structure functions, including “intrinsic" strangeness and charm fluctuations specific to the hadron’s structure rather than gluon substructure [20, 21]. Ladder relations connecting state of different particle number follow from the QCD equation of motion and lead to Regge behavior of the quark and gluon distributions at $x \to 0$ [22].

8. The gauge- and process-independent meson and baryon valence-quark distribution amplitudes $\phi_M(x,Q)$, and $\phi_B(x_i,Q)$ which control exclusive processes involving a hard scale Q, including heavy quark decays, are given by the valence light-front Fock state wavefunctions integrated over the transverse momentum up to the resolution scale Q. The evolution equations for distribution amplitudes follow from the perturbative high transverse momentum behavior of the light-front wavefunctions [9].

9. The line-integrals needed to defining distribution amplitudes and structure functions as gauge invariant matrix elements of operator products vanish in light-front gauge.

10. Proofs of factorization theorems in hard exclusive and inclusive reactions are greatly simplified since the propagating gluons in light-cone gauge couple only to transverse currents; collinear divergences are thus automatically suppressed.

11. At high energies each light-front Fock state interacts distinctly; *e.g.*, Fock states with small particle number and small impact separation have small color dipole moments and can traverse a nucleus with minimal interactions. This is the basis for the predictions for “color transparency" in hard quasi-exclusive [23, 24] and diffractive reactions [2, 3, 4].

12. The Fock state wavefunctions of hadron can be resolved by a high energy diffractive interaction, producing forward jets with momenta which follow the light-front momenta of the wavefunction [2, 3, 4].

13. The deuteron form factor at high Q^2 is sensitive to wavefunction configurations where all six quarks overlap within an impact separation $b_{\perp i} < \mathcal{O}(1/Q)$. The leading power-law fall off predicted by QCD is $F_d(Q^2) = f(\alpha_s(Q^2))/(Q^2)^5$, where, asymptotically, $f(\alpha_s(Q^2)) \propto \alpha_s(Q^2)^{5+2\gamma}$ [25, 26]. In general, the six-quark wavefunction of a deuteron is a mixture of five different color-singlet states. The dominant color configuration at large distances corresponds to the usual proton-neutron bound state. However at small impact space separation, all five Fock color-singlet components eventually evolve to a state with equal weight, *i.e.*, the deuteron wavefunction evolves to 80% “hidden color” [26]. The relatively large normalization of the deuteron form factor observed at large Q^2 hints at sizable hidden-color contributions [27]. Hidden color components can also play a predominant role in the reaction $\gamma d \to J/\psi pn$ at threshold if it is dominated by the multi-fusion process $\gamma gg \to J/\psi$ [28]. Hard exclusive nuclear processes can also be analyzed in terms of “reduced amplitudes" which remove the effects of nucleon substructure.

3. Event Amplitude Generator

The light-cone formalism can provide the foundations for an "event amplitude generator" where each quark and gluon final state is completely labelled in momenta, helicity, and phase. The basic idea is to use the light-cone Hamiltonian P^- to generate the T-matrix in light-cone time-ordered perturbation theory in light-cone gauge. Loop integrals are integrations over the momenta of physical quanta and physical phase space $\prod d^2k_{\perp i} dk_i^+$. The renormalized amplitudes can be explicitly constructed by subtracting from the divergent loops amplitudes with nearly identical integrands corresponding to the contribution of the relevant mass and coupling counter terms (the "alternating denominator method") [29]. The natural renormalization scheme to use for defining the coupling in the event amplitude generator is a physical effective charge such as the pinch scheme [30]. The argument of the coupling is unambiguous. The DLCQ boundary conditions can be used to discretized phase space and limit the number of contributing intermediate states without violating Lorentz invariance. Hadronization processes can be conceivably incorporated by convolution with light-cone wavefunctions. Since one avoids dimensional regularization and nonphysical ghost degrees of freedom, this method of generating events at the amplitude level could be a very simple but powerful tool for simulating events both in QCD and the Standard Model.

4. Other Theoretical Tools

In addition to the light-front Fock expansion, a number of other useful theoretical tools are available to eliminate theoretical ambiguities in QCD predictions:

1. Conformal symmetry provides a template for QCD predictions [31], leading to relations between observables which are present even in a theory which is not scale invariant. For example, the natural representation of distribution amplitudes is in terms of an expansion of orthogonal conformal functions multiplied by anomalous dimensions determined by QCD evolution equations [32, 33, 34]. Thus an important guide in QCD analyses is to identify the underlying conformal relations of QCD which are manifest if we drop quark masses and effects due to the running of the QCD couplings. In fact, if QCD has an infrared fixed point (vanishing of the Gell-Mann-Low function at low momenta), the theory will closely resemble a scale-free conformally symmetric theory in many applications.

2. Commensurate scale relations [35, 36] are perturbative QCD predictions which relate observable to observable at fixed relative scale, such as the "generalized Crewther relation" [37], which connects the Bjorken and Gross-Llewellyn Smith deep inelastic scattering sum rules to measurements of the e^+e^- annihilation cross section. Such relations have no renormalization scale or scheme ambiguity. The coefficients in the perturbative series for commensurate scale relations are identical to those of conformal QCD; thus no infrared renormalons are present [31]. One can identify the required conformal coefficients at any finite order by expanding the coefficients of the usual PQCD expansion around a formal infrared fixed point, as in the Banks-Zak method [38]. All non-conformal effects are absorbed by fixing the ratio of the respective momentum transfer and energy scales. In the case of fixed-point theories, commensurate scale relations relate both the ratio of couplings and the ratio of scales as the fixed point is approached [31].

3. α_V and Skeleton Schemes. A physically natural scheme for defining the QCD coupling in exclusive and other processes is the $\alpha_V(Q^2)$ scheme defined from the potential of static heavy quarks. Heavy-quark lattice gauge theory can provide highly precise values for the coupling. All vacuum polarization corrections due to fermion pairs are then automatically and analytically incorporated into the Gell-Mann-Low function, thus avoiding the problem of explicitly computing and resumming quark mass corrections related to the running of the coupling [39]. The use of a finite effective charge such as α_V as the expansion parameter also provides a basis for regulating the infrared nonperturbative domain of the QCD coupling. A similar coupling and scheme can be based on an assumed skeleton expansion of the theory [30, 38].

4. The Abelian Correspondence Principle. One can consider QCD predictions as analytic functions of the number of colors N_C and flavors N_F. In particular, one can show at all orders of perturbation theory that PQCD predictions reduce to those of an Abelian theory at $N_C \to 0$ with $\hat{\alpha} = C_F \alpha_s$ and $\hat{N}_F = 2N_F/C_F$ held fixed [40]. There is thus a deep connection between QCD processes and their corresponding QED analogs.

5. Other Applications of Light-Front Wavefunctions

Exclusive semileptonic B-decay amplitudes such as $B \to A\ell\overline{\nu}$ can also be evaluated exactly in the light-front formalism [15]. The time-like decay matrix elements require the computation of the diagonal matrix element $n \to n$ where parton number is conserved, and the off-diagonal $n+1 \to n-1$ convolution where the current operator annihilates a $q\overline{q'}$ pair in the initial B wavefunction. This term is a consequence of the fact that the time-like decay $q^2 = (p_\ell + p_{\overline{\nu}})^2 > 0$ requires a positive light-front momentum fraction $q^+ > 0$. Conversely for space-like currents, one can choose $q^+ = 0$, as in the Drell-Yan-West representation of the space-like electromagnetic form factors. However, as can be seen from the explicit analysis of the form factor in a perturbative model, the off-diagonal convolution can yield a nonzero q^+/q^+ limiting form as $q^+ \to 0$. This extra term appears specifically in the case of "bad" currents such as J^- in which the coupling to $q\overline{q}$ fluctuations in the light-front wavefunctions are favored. In effect, the $q^+ \to 0$ limit generates $\delta(x)$ contributions as residues of the $n+1 \to n-1$ contributions. The necessity for such "zero mode" $\delta(x)$ terms was first noted by Chang, Root and Yan [41], Burkardt [42], and Ji and Choi [43].

The off-diagonal $n+1 \to n-1$ contributions give a new perspective for the physics of B-decays. A semileptonic decay involves not only matrix elements where a quark changes flavor, but also a contribution where the leptonic pair is created from the annihilation of a $q\overline{q'}$ pair within the Fock states of the initial B wavefunction. The semileptonic decay thus can occur from the annihilation of a nonvalence quark-antiquark pair in the initial hadron. This feature will carry over to exclusive hadronic B-decays, such as $B^0 \to \pi^- D^+$. In this case the pion can be produced from the coalescence of a $d\overline{u}$ pair emerging from the initial higher particle number Fock wavefunction of the B. The D meson is then formed from the remaining quarks after the internal exchange of a W boson.

In principle, a precise evaluation of the hadronic matrix elements needed for B-decays and other exclusive electroweak decay amplitudes requires knowledge of all of the light-front Fock wavefunctions of the initial and final state hadrons. In the case of model gauge theories such as QCD(1+1) [44] or collinear QCD [45] in one-space and one-time dimensions, the complete evaluation of the light-front wavefunction is possible for each baryon or meson bound-state using the DLCQ method.

The virtual Compton scattering process $\frac{d\sigma}{dt}(\gamma^* p \to \gamma p)$ for large initial photon virtuality $q^2 = -Q^2$ has extraordinary sensitivity to fundamental features of the proton's structure. Even though the final state photon is on-shell, the deeply virtual process probes the elementary quark structure of the proton near the light cone as an effective local current. In contrast to deep inelastic scattering, which measures only the absorptive part of the forward virtual Compton amplitude $Im\mathcal{T}_{\gamma^* p \to \gamma^* p}$, deeply virtual Compton scattering allows the measurement of the phase and spin structure of proton matrix elements for general momentum transfer squared t. In addition, the interference of the virtual Compton amplitude and Bethe-Heitler wide angle scattering Bremsstrahlung amplitude where the photon is emitted from the lepton line leads to an electron-positron asymmetry in the $e^\pm p \to e^\pm \gamma p$ cross section which is proportional to the real part of the Compton amplitude [46, 47, 48]. The deeply virtual Compton amplitude $\gamma^* p \to \gamma p$ is related by crossing to another important process $\gamma^*\gamma \to$ hadron pairs at fixed invariant mass which can be measured in electron-photon collisions [49].

In the handbag approximation, the deeply virtual Compton scattering amplitude $\gamma^*(q)p(P) \to \gamma(q')p(P')$ factorizes as the convolution in x of the amplitude $t^{\mu\nu}$ for hard Compton scattering on a quark line with the generalized Compton form factors $H(x,t,\zeta)$, $E(x,t,\zeta)$, $\widetilde{H}(x,t,\zeta)$, and $\widetilde{E}(x,t,\zeta)$ of the target proton [50, 51, 52, 53, 54, 55, 56, 57, 58, 59, 60, 61]. Here x is the light-front momentum fraction of the struck quark, and $\zeta = Q^2/2P\cdot q$ plays the role of the Bjorken variable. The square of the four-momentum transfer from the proton is given by $t = \Delta^2 = 2P\cdot\Delta =$

$-\frac{(\zeta^2 M^2+\vec{\Delta}_\perp^2)}{(1-\zeta)}$, where Δ is the difference of initial and final momenta of the proton ($P = P' + \Delta$). We will be interested in deeply virtual Compton scattering where q^2 is large compared to the masses and t. Then, to leading order in $1/Q^2$, $\frac{-q^2}{2P_I\cdot q} = \zeta$. Thus ζ plays the role of the Bjorken variable in deeply virtual Compton scattering. For a fixed value of $-t$, the allowed range of ζ is given by

$$0 \;\le\; \zeta \;\le\; \frac{(-t)}{2M^2}\;\left(\sqrt{1+\frac{4M^2}{(-t)}}\;-\;1\right). \tag{3}$$

The form factor $H(x,t,\zeta)$ describes the proton response when the helicity of the proton is unchanged, and $E(x,t,\zeta)$ is for the case when the proton helicity is flipped. Two additional functions $\tilde{H}(x,t,\zeta)$, and $\tilde{E}(x,t,\zeta)$ appear, corresponding to the dependence of the Compton amplitude on quark helicity.

Recently, Markus Diehl, Dae Sung Hwang and I [16] have shown how the deeply virtual Compton amplitude can be evaluated explicitly in the Fock state representation using the matrix elements of the currents and the boost properties of the light-front wavefunctions. For the $n \to n$ diagonal term ($\Delta n = 0$), the arguments of the final-state hadron wavefunction are $\frac{x_1-\zeta}{1-\zeta}$, $\vec{k}_{\perp 1} - \frac{1-x_1}{1-\zeta}\vec{\Delta}_\perp$ for the struck quark and $\frac{x_i}{1-\zeta}$, $\vec{k}_{\perp i} + \frac{x_i}{1-\zeta}\vec{\Delta}_\perp$ for the $n-1$ spectators. As in the case of leptonic B decays, one also the evaluation of an $n+1 \to n-1$ off-diagonal term ($\Delta n = -2$), where partons 1 and $n+1$ of the initial wavefunction annihilate into the current leaving $n-1$ spectators. Then $x_{n+1} = \zeta - x_1$, $\vec{k}_{\perp n+1} = \vec{\Delta}_\perp - \vec{k}_{\perp 1}$. The remaining $n-1$ partons have total momentum $((1-\zeta)P^+, -\vec{\Delta}_\perp)$. The final wavefunction then has arguments $x'_i = \frac{x_i}{1-\zeta}$ and $\vec{k}'_{\perp i} = \vec{k}_{\perp i} + \frac{x_i}{1-\zeta}\vec{\Delta}_\perp$.

6. Applications of QCD Factorization to Hard QCD Processes

Factorization theorems for hard exclusive, semi-exclusive, and diffractive processes allow the separation of soft non-perturbative dynamics of the bound state hadrons from the hard dynamics of a perturbatively-calculable quark-gluon scattering amplitude. The factorization of inclusive reactions is reviewed in ref. For reviews and bibliography of exclusive process calculations in QCD (see Ref. [9, 62]).

The light-front formalism provides a physical factorization scheme which conveniently separates and factorizes soft non-perturbative physics from hard perturbative dynamics in both exclusive and inclusive reactions [5, 63].

In hard inclusive reactions all intermediate states are divided according to $\mathcal{M}_n^2 < \Lambda^2$ and $\mathcal{M}_n^2 > \Lambda^2$ domains. The lower mass regime is associated with the quark and gluon distributions defined from the absolute squares of the LC wavefunctions in the light cone factorization scheme. In the high invariant mass regime, intrinsic transverse momenta can be ignored, so that the structure of the process at leading power has the form of hard scattering on collinear quark and gluon constituents, as in the parton model. The attachment of gluons from the LC wavefunction to a propagator in a hard subprocess is power-law suppressed in LC gauge, so that the minimal quark-gluon particle-number subprocesses dominate. It is then straightforward to derive the DGLAP equations from the evolution of the distributions with $\log\Lambda^2$. The anomaly contribution to singlet helicity structure function $g_1(x,Q)$ can be explicitly identified in the LC factorization scheme as due to the $\gamma^* g \to q\bar{q}$ fusion process. The anomaly contribution would be zero if the gluon is on shell. However, if the off-shellness of the state is larger than the quark pair mass, one obtains the usual anomaly contribution [64].

In exclusive amplitudes, the LC wavefunctions are the interpolating amplitudes connecting the quark and gluons to the hadronic states. In an exclusive amplitude involving a hard scale Q^2 all intermediate states can be divided according to $\mathcal{M}_n^2 < \Lambda^2 < Q^2$ and $\mathcal{M}_n^2 < \Lambda^2$ invariant mass domains. The high invariant mass contributions to the amplitude has the structure of a hard scattering process T_H in which the hadrons are replaced by their respective (collinear) quarks and gluons. In light-cone gauge only the minimal Fock states contribute to the leading power-law fall-off of the exclusive amplitude. The wavefunctions in the lower invariant mass domain can be integrated up to an arbitrary intermediate invariant mass cutoff Λ. The invariant mass domain beyond this cutoff is included in the hard scattering amplitude T_H. The T_H satisfy dimensional counting rules [65]. Final-state and initial state corrections from gluon attachments

to lines connected to the color-singlet distribution amplitudes cancel at leading twist. Explicit examples of perturbative QCD factorization will be discussed in more detail in the next section.

The key non-perturbative input for exclusive processes is thus the gauge and frame independent hadron distribution amplitude [5, 63] defined as the integral of the valence (lowest particle number) Fock wavefunction; *e.g.* for the pion

$$\phi_\pi(x_i,\Lambda) \equiv \int d^2k_\perp\, \psi^{(\Lambda)}_{q\bar{q}/\pi}(x_i,\vec{k}_{\perp i},\lambda) \tag{4}$$

where the global cutoff Λ is identified with the resolution Q. The distribution amplitude controls leading-twist exclusive amplitudes at high momentum transfer, and it can be related to the gauge-invariant Bethe-Salpeter wavefunction at equal light-cone time. The logarithmic evolution of hadron distribution amplitudes $\phi_H(x_i,Q)$ can be derived from the perturbatively-computable tail of the valence light-front wavefunction in the high transverse momentum regime [5, 63]. The conformal basis for the evolution of the three-quark distribution amplitudes for the baryons [66] has recently been obtained by V. Braun *et al.* [34]

The existence of an exact formalism provides a basis for systematic approximations and a control over neglected terms. For example, one can analyze exclusive semi-leptonic B-decays which involve hard internal momentum transfer using a perturbative QCD formalism [6, 7, 67, 68, 69, 70] patterned after the perturbative analysis of form factors at large momentum transfer. The hard-scattering analysis again proceeds by writing each hadronic wavefunction as a sum of soft and hard contributions

$$\psi_n = \psi_n^{\rm soft}(\mathcal{M}_n^2 < \Lambda^2) + \psi_n^{\rm hard}(\mathcal{M}_n^2 > \Lambda^2), \tag{5}$$

where $\mathcal{M}_n^2$ is the invariant mass of the partons in the n-particle Fock state and Λ is the separation scale. The high internal momentum contributions to the wavefunction $\psi_n^{\rm hard}$ can be calculated systematically from QCD perturbation theory by iterating the gluon exchange kernel. The contributions from high momentum transfer exchange to the B-decay amplitude can then be written as a convolution of a hard-scattering quark-gluon scattering amplitude T_H with the distribution amplitudes $\phi(x_i,\Lambda)$, the valence wavefunctions obtained by integrating the constituent momenta up to the separation scale $\mathcal{M}_n < \Lambda < Q$. Furthermore in processes such as $B \to \pi D$ where the pion is effectively produced as a rapidly-moving small Fock state with a small color-dipole interactions, final state interactions are suppressed by color transparency. This is the basis for the perturbative hard-scattering analyses [6, 7, 67, 69, 70]. In a systematic analysis, one can identify the hard PQCD contribution as well as the soft contribution from the convolution of the light-front wavefunctions. Furthermore, the hard-scattering contribution can be systematically improved.

Given the solution for the hadronic wavefunctions $\psi_n^{(\Lambda)}$ with $\mathcal{M}_n^2 < \Lambda^2$, one can construct the wavefunction in the hard regime with $\mathcal{M}_n^2 > \Lambda^2$ using projection operator techniques. The construction can be done perturbatively in QCD since only high invariant mass, far off-shell matrix elements are involved. One can use this method to derive the physical properties of the LC wavefunctions and their matrix elements at high invariant mass. Since $\mathcal{M}_n^2 = \sum_{i=1}^n \left(\frac{k_\perp^2+m^2}{x}\right)_i$, this method also allows the derivation of the asymptotic behavior of light-front wavefunctions at large $k_\perp$, which in turn leads to predictions for the fall-off of form factors and other exclusive matrix elements at large momentum transfer, such as the quark counting rules for predicting the nominal power-law fall-off of two-body scattering amplitudes at fixed θ_{cm} [65] and helicity selection rules [71]. The phenomenological successes of these rules can be understood within QCD if the coupling $\alpha_V(Q)$ freezes in a range of relatively small momentum transfer [72].

7. Two-Photon Processes

The simplest and perhaps the most elegant illustration of an exclusive reaction in QCD is the evaluation of the photon-to-pion transition form factor $F_{\gamma\to\pi}(Q^2)$ [5, 73] which is measurable in single-tagged two-photon $ee \to ee\pi^0$ reactions. The form factor is defined via the invariant amplitude $\Gamma^\mu = -ie^2F_{\pi\gamma}(Q^2)\varepsilon^{\mu\nu\rho\sigma}p_\nu^\pi\varepsilon_\rho q_\sigma$. As in inclusive reactions, one must specify a factorization scheme which divides the integration regions of the loop integrals into hard and soft momenta, compared to the resolution scale $\widetilde{Q}$. At leading twist, the transition form factor then factorizes

as a convolution of the $\gamma^*\gamma \to q\overline{q}$ amplitude (where the quarks are collinear with the final state pion) with the valence light-front wavefunction of the pion:

$$F_{\gamma M}(Q^2) = \frac{4}{\sqrt{3}} \int_0^1 dx \phi_M(x, \widetilde{Q}) T^H_{\gamma\to M}(x, Q^2). \tag{6}$$

The hard scattering amplitude for $\gamma\gamma^* \to q\overline{q}$ is $T^H_{\gamma M}(x, Q^2) = [(1-x)Q^2]^{-1} \times (1 + \mathcal{O}(\alpha_s))$. The leading QCD corrections have been computed by Braaten [74]. The evaluation of the next-to-leading corrections in the physical α_V scheme is given in Ref. [72]. For the asymptotic distribution amplitude $\phi_\pi^{\rm asympt}(x) = \sqrt{3} f_\pi x(1-x)$ one predicts $Q^2 F_{\gamma\pi}(Q^2) = 2 f_\pi \left(1 - \frac{5}{3}\frac{\alpha_V(Q^*)}{\pi}\right)$ where $Q^* = e^{-3/2}Q$ is the BLM scale for the pion form factor. The PQCD predictions have been tested in measurements of $e\gamma \to e\pi^0$ by the CLEO collaboration [75]. The observed flat scaling of the $Q^2 F_{\gamma\pi}(Q^2)$ data from $Q^2 = 2$ to $Q^2 = 8$ GeV^2 provides an important confirmation of the applicability of leading twist QCD to this process. The magnitude of $Q^2 F_{\gamma\pi}(Q^2)$ is remarkably consistent with the predicted form, assuming the asymptotic distribution amplitude and including the LO QCD radiative correction with $\alpha_V(e^{-3/2}Q)/\pi \simeq 0.12$. One could allow for some broadening of the distribution amplitude with a corresponding increase in the value of α_V at small scales. Radyushkin [76], Ong [77], and Kroll [78] have also noted that the scaling and normalization of the photon-to-pion transition form factor tends to favor the asymptotic form for the pion distribution amplitude and rules out broader distributions such as the two-humped form suggested by QCD sum rules [79].

The two-photon annihilation process $\gamma^*\gamma \to$ hadrons, which is measurable in single-tagged $e^+e^- \to e^+e^-$hadrons events, provides a semi-local probe of $C = +$ hadron systems $\pi^0, \eta^0, \eta', \eta_c, \pi^+\pi^-$, etc. The $\gamma^*\gamma \to \pi^+\pi^-$ hadron pair process is related to virtual Compton scattering on a pion target by crossing. The leading twist amplitude is sensitive to the $1/x - 1/(1-x)$ moment of the two-pion distribution amplitude coupled to two valence quarks [49, 80].

Two-photon reactions, $\gamma\gamma \to H\overline{H}$ at large s $= (k_1 + k_2)^2$ and fixed $\theta_{\rm cm}$, provide a particularly important laboratory for testing QCD since these cross-channel "Compton" processes are the simplest calculable large-angle exclusive hadronic scattering reactions. The helicity structure, and often even the absolute normalization can be rigorously computed for each two-photon channel [73]. In the case of meson pairs, dimensional counting predicts that for large s, $s^4 d\sigma/dt(\gamma\gamma \to M\overline{M}$ scales at fixed t/s or $\theta_{\rm c.m.}$ up to factors of $\ln s/\Lambda^2$. The angular dependence of the $\gamma\gamma \to H\overline{H}$ amplitudes can be used to determine the shape of the process-independent distribution amplitudes, $\phi_H(x, Q)$. An important feature of the $\gamma\gamma \to M\overline{M}$ amplitude for meson pairs is that the contributions of Landshoff pitch singularities are power-law suppressed at the Born level – even before taking into account Sudakov form factor suppression. There are also no anomalous contributions from the $x \to 1$ endpoint integration region. Thus, as in the calculation of the meson form factors, each fixed-angle helicity amplitude can be written to leading order in $1/Q$ in the factorized form [$Q^2 = p_T^2 = tu/s; \widetilde{Q}_x = \min(xQ, (l-x)Q)$]:

$$\mathcal{M}_{\gamma\gamma\to M\overline{M}} = \int_0^1 dx \int_0^1 dy \phi_{\overline{M}}(y, \widetilde{Q}_y) T_H(x, y, s, \theta_{\rm c.m.} \phi_M(x, \widetilde{Q}_x), \tag{7}$$

where T_H is the hard-scattering amplitude $\gamma\gamma \to (q\overline{q})(q\overline{q})$ for the production of the valence quarks collinear with each meson, and $\phi_M(x, \widetilde{Q})$ is the amplitude for finding the valence q and $\overline{q}$ with light-front fractions of the meson's momentum, integrated over transverse momenta $k_\perp < \widetilde{Q}$. The contribution of non-valence Fock states are power-law suppressed. Furthermore, the helicity-selection rules [71] of perturbative QCD predict that vector mesons are produced with opposite helicities to leading order in $1/Q$ and all orders in α_s. The dependence in x and y of several terms in $T_{\lambda,\lambda'}$ is quite similar to that appearing in the meson's electromagnetic form factor. Thus much of the dependence on $\phi_M(x, Q)$ can be eliminated by expressing it in terms of the meson form factor. In fact, the ratio of the $\gamma\gamma \to \pi^+\pi^-$ and $e^+e^- \to \mu^+\mu^-$ amplitudes at large s and fixed θ_{CM} is nearly insensitive to the running coupling and the shape of the pion distribution amplitude:

$$\frac{\frac{d\sigma}{dt}(\gamma\gamma \to \pi^+\pi^-)}{\frac{d\sigma}{dt}(\gamma\gamma \to \mu^+\mu^-)} \sim \frac{4|F_\pi(s)|^2}{1 - \cos^2\theta_{\rm c.m.}}. \tag{8}$$

The comparison of the PQCD prediction for the sum of $\pi^+\pi^-$ plus K^+K^- channels with recent CLEO data [81] is shown in Fig. 1. The CLEO data for charged pion and kaon pairs show a clear transition to the scaling and angular distribution predicted by PQCD [73] for $W = \sqrt{(s_{\gamma\gamma}} > 2$ GeV. It is clearly important to measure the magnitude and angular dependence of the two-photon production of neutral pions and $\rho^+\rho^-$ cross sections in view of the strong sensitivity of these channels to the shape of meson distribution amplitudes. QCD also predicts that the production cross section for charged ρ-pairs (with any helicity) is much larger that for that of neutral ρ pairs, particularly at large $\theta_{\rm c.m.}$ angles. Similar predictions are possible for other helicity-zero mesons. The cross sections for Compton scattering on protons and the crossed reaction $\gamma\gamma \to p\overline{p}$ at high momentum transfer have also been evaluated [82, 83], providing important tests of the proton distribution amplitude.

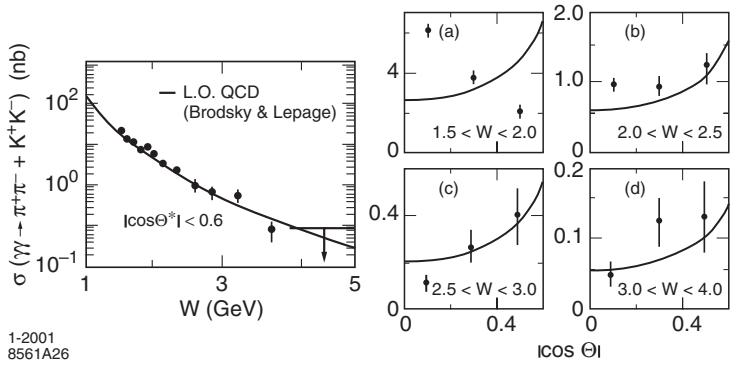

Figure 1: Comparison of the sum of $\gamma\gamma \to \pi^+\pi^-$ and $\gamma\gamma \to K^+K^-$ meson pair production cross sections with the scaling and angular distribution of the perturbative QCD prediction [73]. The data are from the CLEO collaboration [81].

It is particularly compelling to see a transition in angular dependence between the low energy chiral and PQCD regimes. The success of leading-twist perturbative QCD scaling for exclusive processes at presently experimentally accessible momentum transfer can be understood if the effective coupling $\alpha_V(Q^*)$ is approximately constant at the relatively small scales Q^* relevant to the hard scattering amplitudes [72]. The evolution of the quark distribution amplitudes In the low-Q^* domain at also needs to be minimal. Sudakov suppression of the endpoint contributions is also strengthened if the coupling is frozen because of the exponentiation of a double logarithmic series.

Clearly much more experimental input on hadron wavefunctions is needed, particularly from measurements of two-photon exclusive reactions into meson and baryon pairs at the high luminosity B factories. For example, the ratio $\frac{d\sigma}{dt}(\gamma\gamma \to \pi^0\pi^0)/\frac{d\sigma}{dt}(\gamma\gamma \to \pi^+\pi^-)$ is particularly sensitive to the shape of pion distribution amplitude. Baryon pair production in two-photon reactions at threshold may reveal physics associated with the soliton structure of baryons in QCD [84, 85]. In addition, fixed target experiments can provide much more information on fundamental QCD processes such as deeply virtual Compton scattering and large angle Compton scattering.

8. Diffraction and Light-Cone Wavefunctions

The diffractive dissociation of a hadron at high energies, by either Coulomb or Pomeron exchange, can be understood as the materialization of the projectile's light-cone wavefunctions; in particular, the diffractive dissociation of a meson, baryon, or photon into high transverse momentum jets measures the shape and other features of the projectile's distribution amplitude, $\phi(x_i, Q)$, the valence wavefunction which controls high momentum transfer exclusive amplitudes. Diffractive dissociation can also test fundamental properties of QCD, including color transparency and intrinsic charm.

Diffractive dissociation in QCD can be understood as a three-step process:

1. The initial hadron can be decomposed in terms of its quark and gluon constituents in terms of its light-cone Fock-state wavefunctions.

2. In the second step, the incoming hadron is resolved by Pomeron or Odderon (multi-gluon) exchange with the target or by Coulomb dissociation. The exchanged interaction has to supply sufficient momentum transfer q^μ to put the diffracted state X on shell. Light-cone energy conservation requires $q^- = (m_X^2 - m_\pi^2)/P_\pi^+$, where m_X is the invariant mass of X. In a heavy target rest system, the longitudinal momentum transfer for a pion beam is $q^z = (m_X^2 - m_\pi^2)/E_{\pi\text{lab}}$. Thus the momentum transfer $t = q^2$ to the target can be sufficiently small so that the target remains intact.

   In perturbative QCD, the pomeron is generally be represented as multiple gluon exchange between the target and projectile. Effectively this interaction occurs over a short light-cone time interval, and thus like photon exchange, the perturbative QCD pomeron can be effectively represented as a local operator. This description is believed to be applicable when the pomeron has to resolve compact states and is the basis for the terminology "hard pomeron". The BFKL formalism generalizes the perturbative QCD treatment by an all-orders perturbative resummation, generating a pomeron with a fixed Regge intercept $\alpha_P(0)$. Next to leading order calculations with BLM scale fixing leads to a predicted intercept $\alpha_P(0) \simeq 0.4$ [86]. However, when the exchange interactions are soft, a multiperipheral description in terms of meson ladders may dominate the physics. This is the basis for the two-component pomeron model of Donnachie and Landshoff [87].

   Consider a collinear frame where the incident momentum P_π^+ is large and $s = (p_\pi + p_{\text{target}})^2 \simeq p_\pi^+ p_{\text{target}}^-$. The matrix element of an exchanged gluon with momentum q_i between the projectile and an intermediate state $|N\rangle$ is dominated by the "plus current": $\left\langle \pi | j^+(0) \exp(i\frac{1}{2} q_i^+ x^- - i q_{\perp i} \cdot x_\perp | N \right\rangle$. Note that the coherent sum of couplings of an exchanged gluon to the pion system vanishes when its momentum is small compared to the characteristic momentum scales in the projectile light-cone wavefunction: $q^{\perp i} \Delta x_\perp \ll 1$ and $q_i^+ \Delta x^- \ll 1$. The destructive interference of the gauge couplings to the constituents of the projectile follows simply from the fact that the color charge operator has zero matrix element between distinct eigenstates of the QCD Hamiltonian: $\langle A|Q|B\rangle \equiv \int d^2x_\perp dx^- \langle A|j^+(0)|B\rangle = 0$ [88]. At high energies the change in k_i^+ of the constituents can be ignored, so that Fock states of a hadron with small transverse size interact weakly even in a nuclear target because of their small dipole moment. This is the basis of "color transparency" in perturbative QCD [2, 23]. To a good approximation the sum of couplings to the constituents of the projectile can be represented as a derivative with respect to transverse momentum. Thus photon exchange measures a weighted sum of transverse derivatives $\partial_{k_\perp} \psi_n(x_i, k_{\perp i}, \lambda_i)$, and two-gluon exchange measures the second transverse partial derivative [89].

3. The final step is the hadronization of the n constituents of the projectile Fock state into final state hadrons. Since q_i^+ is small, the number of partons in the initial Fock state and the final state hadrons are unchanged. Their coalescence is thus governed by the convolution of initial and final-state Fock state wavefunctions. In the case of states with high $k_\perp$, the final state will hadronize into jets, each reflecting the respective x_i of the Fock state constituents. In the case of higher Fock states with intrinsic sea quarks such as an extra $c\bar{c}$ pair (intrinsic charm), one will observe leading J/ψ or open charm hadrons in the projectile fragmentation region; *i.e.*, the hadron's fragments will tend to have the same rapidity as that of the projectile.

For example, diffractive multi-jet production in heavy nuclei provides a novel way to measure the shape of the LC Fock state wavefunctions and test color transparency. Consider the reaction [2, 3, 90] $\pi A \to \text{Jet}_1 + \text{Jet}_2 + A'$ at high energy where the nucleus A' is left intact in its ground state. The transverse momenta of the jets balance so that $\vec{k}_{\perp i} + \vec{k}_{\perp 2} = \vec{q}_\perp < R^{-1}{}_A$. The light-front longitudinal momentum fractions also need to add to $x_1 + x_2 \sim 1$ so that $\Delta p_L < R_A^{-1}$. The process can then occur coherently in the nucleus. Because of color transparency, the valence wavefunction of the pion with small impact separation, will penetrate the nucleus with minimal interactions, diffracting into jet pairs [2]. The $x_1 = x$, $x_2 = 1 - x$ dependence of the di-jet distributions will thus reflect the shape of the pion valence light-front wavefunction in x; similarly, the $\vec{k}_{\perp 1} - \vec{k}_{\perp 2}$ relative transverse momenta of the jets gives key information on the second derivative of the underlying shape of the valence pion wavefunction [3, 89, 90]. The diffractive nuclear amplitude

extrapolated to $t = 0$ should be linear in nuclear number A if color transparency is correct. The integrated diffractive rate should then scale as $A^2/R_A^2 \sim A^{4/3}$.

The results of a diffractive dijet dissociation experiment of this type E791 at Fermilab using 500 GeV incident pions on nuclear targets [91] appear to be consistent with color transparency. The measured longitudinal momentum distribution of the jets [92] is consistent with a pion light-cone wavefunction of the pion with the shape of the asymptotic distribution amplitude, $\phi_\pi^{\rm asympt}(x) = \sqrt{3} f_\pi x(1-x)$. Data from CLEO [75] for the $\gamma\gamma^* \to \pi^0$ transition form factor also favor a form for the pion distribution amplitude close to the asymptotic solution to the perturbative QCD evolution equation [5].

The interpretation of the diffractive dijet processes as measures of the hadron distribution amplitudes has recently been questioned by Braun *et al.* [93] and by Chernyak [94] who have calculated the hard scattering amplitude for such processes at next-to-leading order. However, these analyses neglect the integration over the transverse momentum of the valence quarks and thus miss the logarithmic ordering which is required for factorization of the distribution amplitude and color-filtering in nuclear targets.

As noted above, the diffractive dissociation of a hadron or nucleus can also occur via the Coulomb dissociation of a beam particle on an electron beam (*e.g.* at HERA or eRHIC) or on the strong Coulomb field of a heavy nucleus (*e.g.* at RHIC or nuclear collisions at the LHC) [89]. The amplitude for Coulomb exchange at small momentum transfer is proportional to the first derivative $\sum_i e_i \frac{\partial}{\vec{k}_{Ti}} \psi$ of the light-front wavefunction, summed over the charged constituents. The Coulomb exchange reactions fall off less fast at high transverse momentum compared to pomeron exchange reactions since the light-front wavefunction is effective differentiated twice in two-gluon exchange reactions.

It will also be interesting to study diffractive tri-jet production using proton beams $pA \to {\rm Jet}_1 + {\rm Jet}_2 + {\rm Jet}_3 + A'$ to determine the fundamental shape of the 3-quark structure of the valence light-front wavefunction of the nucleon at small transverse separation [3]. For example, consider the Coulomb dissociation of a high energy proton at HERA. The proton can dissociate into three jets corresponding to the three-quark structure of the valence light-front wavefunction. We can demand that the produced hadrons all fall outside an opening angle θ in the proton's fragmentation region. Effectively all of the light-front momentum $\sum_j x_j \simeq 1$ of the proton's fragments will thus be produced outside an "exclusion cone". This then limits the invariant mass of the contributing Fock state $M_n^2 > \Lambda^2 = P^{+2} \sin^2\theta/4$ from below, so that perturbative QCD counting rules can predict the fall-off in the jet system invariant mass M. The segmentation of the forward detector in azimuthal angle ϕ can be used to identify structure and correlations associated with the three-quark light-front wavefunction [89]. One can use also measure the dijet structure of real and virtual photons beams $\gamma^* A \to {\rm Jet}_1 + {\rm Jet}_2 + A'$ to measure the shape of the light-front wavefunction for transversely-polarized and longitudinally-polarized virtual photons. Such experiments will open up a direct window on the amplitude structure of hadrons at short distances. The light-front formalism is also applicable to the description of nuclei in terms of their nucleonic and mesonic degrees of freedom [95, 96]. Self-resolving diffractive jet reactions in high energy electron-nucleus collisions and hadron-nucleus collisions at moderate momentum transfers can thus be used to resolve the light-front wavefunctions of nuclei.

Thus diffractive jet production can provide direct empirical information on the light-front wavefunctions of hadrons. The E791 experiment at Fermilab has not only determined the main features of the pion wavefunction, but has also confirmed color transparency, a fundamental test of the gauge properties of QCD. Analogous reaction involving nuclear projectiles can resolve the light-front wavefunctions of nuclei in terms of their nucleon and mesonic degrees of freedom. It is also possible to measure the light-front wavefunctions of atoms through high energy Coulomb dissociation.

9. Heavy Quark Fluctuations in Diffractive Dissociation

Since a hadronic wavefunction describes states off of the light-cone energy shell, there is a finite probability of the projectile having fluctuations containing extra quark-antiquark pairs, such as intrinsic strangeness charm, and bottom. In contrast to the quark pairs arising from gluon splitting, intrinsic quarks are multiply-connected to the valence quarks and are thus part of the dynamics of the hadron. Recently Franz, Polyakov, and Goeke have analyzed the properties of

the intrinsic heavy-quark fluctuations in hadrons using the operator-product expansion [97]. For example, the light-cone momentum fraction carried by intrinsic heavy quarks in the proton $x_{Q\overline{Q}}$ as measured by the T^{++} component of the energy-momentum tensor is related in the heavy-quark limit to the forward matrix element $\langle p|\mathrm{tr}_c(G^{+\alpha}G^{+\beta}G_{\alpha\beta})/m_Q^2|p\rangle$, where $G^{\mu\nu}$ is the gauge field strength tensor. Diagrammatically, this can be described as a heavy quark loop in the proton self-energy with four gluons attached to the light, valence quarks. Since the non-Abelian commutator $[A_\alpha, A_\beta]$ is involved, the heavy quark pairs in the proton wavefunction are necessarily in a color-octet state. It follows from dimensional analysis that the momentum fraction carried by the $Q\overline{Q}$ pair scales as $k_\perp^2/m_Q^2$ where $k_\perp$ is the typical momentum in the hadron wave function. [In contrast, in the case of Abelian theories, the contribution of an intrinsic, heavy lepton pair to the bound state's structure first appears in $O(1/m_L^4)$. One relevant operator corresponds to the Born-Infeld $(F_{\mu\nu})^4$ light-by-light scattering insertion, and the momentum fraction of heavy leptons in an atom scales as $k_\perp^4/m_L^4$.]

Intrinsic charm can be materialized by diffractive dissociation into open or hidden charm states such as $pp \to J/\psi X p', \Lambda_c X p'$. At HERA one can measure intrinsic charm in the proton by Coulomb dissociation: $pe \to \Lambda_C X e'$, and $J/\psi X e'$. Since the intrinsic heavy quarks tend to have the same rapidity as that of the projectile, they are produced at large x_F in the beam fragmentation region. The charm structure function measured by the EMC group shows an excess at large x_{bj}, indicating a probability of order 1% for intrinsic charm in the proton [21]. The presence of intrinsic charm in light-mesons provides an explanation for the puzzle of the large $J/\psi \to \rho\pi$ branching ratio and suppressed $\psi' \to \rho\pi$ decay [98]. The presence of intrinsic charm quarks in the B wave function provides new mechanisms for B decays. For example, Chang and Hou have considered the production of final states with three charmed quarks such as $B \to J/\psi D\pi$ and $B \to J/\psi D^*$ [99]; these final states are difficult to realize in the valence model, yet they occur naturally when the b quark of the intrinsic charm Fock state $|b\overline{u}c\overline{c}\rangle$ decays via $b \to c\overline{u}d$. In fact, the J/ψ spectrum for inclusive $B \to J/\psi X$ decays measured by CLEO and Belle shows a distinct enhancement at the low J/ψ momentum where such decays would kinematically occur. Alternatively, this excess could reflect the opening of baryonic channels such as $B \to J/\psi\overline{p}\Lambda$ [100]. Recently, Susan Gardner and I have shown that the presence of intrinsic charm in the hadrons' light-cone wave functions, even at a few percent level, provides new, competitive decay mechanisms for B decays which are nominally CKM-suppressed [101]. For example, the weak decays of the B-meson to two-body exclusive states consisting of strange plus light hadrons, such as $B \to \pi K$, are expected to be dominated by penguin contributions since the tree-level $b \to su\overline{u}$ decay is CKM suppressed. However, higher Fock states in the B wave function containing charm quark pairs can mediate the decay via a CKM-favored $b \to sc\overline{c}$ tree-level transition. Such intrinsic charm contributions can be phenomenologically significant. Since they mimic the amplitude structure of "charming" penguin contributions [102], charming penguins need not be penguins at all [101].

10. Calculations of Light-Cone Wavefunctions

Is there any hope of computing light-front wavefunctions from first principles? The solution of the light-front Hamiltonian equation $H_{LC}^{QCD}|\Psi\rangle = M^2|\Psi\rangle$ is an eigenvalue problem which in principle determines the masses squared of the entire bound and continuum spectrum of QCD. If one introduces periodic or anti-periodic boundary conditions, the eigenvalue problem is reduced to the diagonalization of a discrete Hermitian matrix representation of H_{LC}^{QCD}. The light-front momenta satisfy $x^+ = \frac{2\pi}{L}n_i$ and $P^+ = \frac{2\pi}{L}K$, where $\sum_i n_i = K$. The number of quanta in the contributing Fock states is restricted by the choice of harmonic resolution. A cutoff on the invariant mass of the Fock states truncates the size of the matrix representation in the transverse momenta. This is the essence of the DLCQ method [103], which has now become a standard tool for solving both the spectrum and light-front wavefunctions of one-space one-time theories – virtually any 1 + 1 quantum field theory, including "reduced QCD" (which has both quark and gluonic degrees of freedom) can be completely solved using DLCQ [45, 104]. The method yields not only the bound-state and continuum spectrum, but also the light-front wavefunction for each eigensolution [105, 106].

In the case of theories in 3+1 dimensions, Hiller, McCartor, and I [107, 108] have recently shown that the use of covariant Pauli-Villars regularization with DLCQ allows one to obtain the spectrum

and light-front wavefunctions of simplified theories, such as (3+1) Yukawa theory. Dalley *et al.* have shown how one can use DLCQ in one space-one time, with a transverse lattice to solve mesonic and gluonic states in 3 + 1 QCD [109]. The spectrum obtained for gluonium states is in remarkable agreement with lattice gauge theory results, but with a huge reduction of numerical effort. Hiller and I [110] have shown how one can use DLCQ to compute the electron magnetic moment in QED without resort to perturbation theory.

One can also formulate DLCQ so that supersymmetry is exactly preserved in the discrete approximation, thus combining the power of DLCQ with the beauty of supersymmetry [111, 112, 113]. The "SDLCQ" method has been applied to several interesting supersymmetric theories, to the analysis of zero modes, vacuum degeneracy, massless states, mass gaps, and theories in higher dimensions, and even tests of the Maldacena conjecture [111]. Broken supersymmetry is interesting in DLCQ, since it may serve as a method for regulating non-Abelian theories [108].

There are also many possibilities for obtaining approximate solutions of light-front wavefunctions in QCD. QCD sum rules, lattice gauge theory moments, and QCD inspired models such as the bag model, chiral theories, provide important constraints. Guides to the exact behavior of LC wavefunctions in QCD can also be obtained from analytic or DLCQ solutions to toy models such as "reduced" $QCD(1+1)$. The light-front and many-body Schrödinger theory formalisms must match In the nonrelativistic limit.

It would be interesting to see if light-front wavefunctions can incorporate chiral constraints such as soliton (Skyrmion) behavior for baryons and other consequences of the chiral limit in the soft momentum regime. Solvable theories such as $QCD(1+1)$ are also useful for understanding such phenomena. It has been shown that the anomaly contribution for the $\pi^0 \to \gamma\gamma$ decay amplitude is satisfied by the light-front Fock formalism in the limit where the mass of the pion is light compared to its size [114].

One can also compute the distribution amplitude from the gauge invariant Bethe-Salpeter wavefunction at equal light-cone time. This also allows contact with both QCD sum rules and lattice gauge theory; for example, moments of the pion distribution amplitudes have been computed in lattice gauge theory [115, 116, 117].

Dalley [118] has recently calculated the pion distribution amplitude from QCD using a combination of the discretized DLCQ method for the x^- and x^+ light-cone coordinates with the transverse lattice method [119, 120] in the transverse directions. A finite lattice spacing a can be used by choosing the parameters of the effective theory in a region of renormalization group stability to respect the required gauge, Poincaré, chiral, and continuum symmetries. The overall normalization gives $f_\pi = 101$ MeV compared with the experimental value of 93 MeV. The resulting DLCQ/transverse lattice pion wavefunction with the best fit to the diffractive di-jet data after corrections for hadronization and experimental acceptance [1]. The predicted form of $\phi_\pi(x,Q)$ is somewhat broader than but not inconsistent with the asymptotic form favored by the measured normalization of $Q^2 F_{\gamma\pi^0}(Q^2)$ and the pion wavefunction inferred from diffractive di-jet production. However, there are experimental uncertainties from hadronization and theoretical errors introduced from finite DLCQ resolution, using a nearly massless pion, ambiguities in setting the factorization scale Q^2, as well as errors in the evolution of the distribution amplitude from 1 to 10 GeV^2.

Instanton models also predict a pion distribution amplitude close to the asymptotic form [121]. In contrast, recent lattice results from Del Debbio *et al.* [116] predict a much narrower shape for the pion distribution amplitude than the distribution predicted by the transverse lattice. A new result for the proton distribution amplitude treating nucleons as chiral solitons has recently been derived by Diakonov and Petrov [122]. Dyson-Schwinger models [123] of hadronic Bethe-Salpeter wavefunctions can also be used to predict light-cone wavefunctions and hadron distribution amplitudes by integrating over the relative k^- momentum. There is also the possibility of deriving Bethe-Salpeter wavefunctions within light-cone gauge quantized QCD [124] in order to properly match to the light-cone gauge Fock state decomposition.

Clearly much more experimental input on hadron wavefunctions is needed, particularly from measurements of two-photon exclusive reactions into meson and baryon pairs at the high luminosity B factories. For example, the ratio $\frac{d\sigma}{dt}(\gamma\gamma \to \pi^0\pi^0)/\frac{d\sigma}{dt}(\gamma\gamma \to \pi^+\pi^-)$ is particularly sensitive to the shape of pion distribution amplitude. Baryon pair production in two-photon reactions at threshold may reveal physics associated with the soliton structure of baryons in QCD [84]. In addition, fixed target experiments can provide much more information on fundamental QCD processes such as deeply virtual Compton scattering and large angle Compton scattering.

There has been notable progress in computing light-front wavefunctions directly from the QCD light-front Hamiltonian, using DLCQ and transverse lattice methods. Even without full non-perturbative solutions of QCD, one can envision a program to construct the light-front wavefunctions using measured moments constraints from QCD sum rules, lattice gauge theory, and data from hard exclusive and inclusive processes. One can also be guided by theoretical constraints from perturbation theory which dictate the asymptotic form of the wavefunctions at large invariant mass, $x \to 1$, and high $k_\perp$. One can also use ladder relations which connect Fock states of different particle number; perturbatively-motivated numerator spin structures; conformal symmetry, guidance from toy models such as "reduced" $QCD(1+1)$; and the correspondence to Abelian theory for $N_C \to 0$, as well as many-body Schrödinger theory in the nonrelativistic domain.

11. Calculating and Modelling Light-Cone Wavefunctions

The discretized light-cone quantization method [125] is a powerful technique for finding the non-perturbative solutions of quantum field theories. The basic method is to diagonalize the light-cone Hamiltonian in a light-cone Fock basis defined using periodic boundary conditions in x^- and $x_\perp$. The method preserves the frame-independence of the front form. The DLCQ method is now used extensively to solve one-space and one-time theories, including supersymmetric theories. New applications of DLCQ to supersymmetric quantum field theories and specific tests of the Maldacena conjecture have recently been given by Pinsky and Trittman. There has been progress in systematically developing the computation and renormalization methods needed to make DLCQ viable for QCD in physical spacetime. For example, John Hiller, Gary McCartor and I [126] have shown how DLCQ can be used to solve 3+1 theories despite the large numbers of degrees of freedom needed to enumerate the Fock basis. A key feature of our work, is the introduction of Pauli Villars fields in order to regulate the UV divergences and perform renormalization while preserving the frame-independence of the theory. A review of DLCQ and its applications is given in Ref. [8]. There has also been important progress using the transverse lattice, essentially a combination of DLCQ in 1+1 dimensions together with a lattice in the transverse dimensions.

Even without explicit solutions, many features of the light-cone wavefunctions follow from general arguments. Light-cone wavefunctions satisfy the equation of motion:

$$H_{LC}^{QCD}|\Psi\rangle = (H_{LC}^0 + V_{LC})|\Psi\rangle = M^2|\Psi\rangle \ , \tag{9}$$

which has the Heisenberg matrix form in Fock space:

$$M^2 - \sum_{i=1}^{n} \frac{m_{\perp i}^2}{x_i}\psi_n = \sum_{n'} \int \langle n|V|n'\rangle \, \psi_{n'} \tag{10}$$

where the convolution and sum is understood over the Fock number, transverse momenta, plus momenta and helicity of the intermediate states. Here $m_\perp^2 = m^2 + k_\perp^2$. Thus, in general, every light-cone Fock wavefunction has the form:

$$\psi_n = \frac{\Gamma_n}{M^2 - \sum_{i=1}^{n} \frac{m_{\perp i}^2}{x_i}} \tag{11}$$

where $\Gamma_n = \sum_{n'} \int V_{nn'}\psi_n$. The main dynamical dependence of a light-cone wavefunction away from the extrema is controlled by its light-cone energy denominator. The maximum of the wavefunction occurs when the invariant mass of the partons is minimal; *i.e.*, when all particles have equal rapidity and are all at rest in the rest frame. In fact, Dae Sung Hwang and I [88] have noted that one can rewrite the wavefunction in the form:

$$\psi_n = \frac{\Gamma_n}{M^2[\sum_{i=1}^{n} \frac{(x_i - \hat{x}_i)^2}{x_i} + \delta^2]} \tag{12}$$

where $x_i = \hat{x}_i \equiv m_{\perp i}/\sum_{i=1}^{n} m_{\perp i}$ is the condition for minimal rapidity differences of the constituents. The key parameter is $M^2 - \sum_{i=1}^{n} m_{\perp i}^2/\hat{x}_i \equiv -M^2\delta^2$. We can also interpret $\delta^2 \simeq 2\varepsilon/M$

where $\varepsilon = \sum_{i=1}^{n} m_{\perp i} - M$ is the effective binding energy. This form shows that the wavefunction is a quadratic form around its maximum, and that the width of the distribution in $(x_i - \hat{x}_i)^2$ (where the wavefunction falls to half of its maximum) is controlled by $x_i \delta^2$ and the transverse momenta $k_{\perp_i}$. Note also that the heaviest particles tend to have the largest $\hat{x}_i$, and thus the largest momentum fraction of the particles in the Fock state, a feature familiar from the intrinsic charm model. For example, the b quark has the largest momentum fraction at small $k_\perp$ in the B meson's valence light-cone wavefunction,, but the distribution spreads out to an asymptotically symmetric distribution around $x_b \sim 1/2$ when $k_\perp \gg m_b^2$.

We can also discern some general properties of the numerator of the light-cone wavefunctions. $\Gamma_n(x_i, k_{\perp i}, \lambda_i)$. The transverse momentum dependence of Γ_n guarantees J_z conservation for each Fock state: Each light-cone Fock wavefunction satisfies conservation of the z projection of angular momentum: $J^z = \sum_{i=1}^{n} S_i^z + \sum_{j=1}^{n-1} l_j^z$. The sum over s_i^z represents the contribution of the intrinsic spins of the n Fock state constituents. The sum over orbital angular momenta $l_j^z = -\mathrm{i}(k_j^1 \frac{\partial}{\partial k_j^2} - k_j^2 \frac{\partial}{\partial k_j^1})$ derives from the $n-1$ relative momenta. This excludes the contribution to the orbital angular momentum due to the motion of the center of mass, which is not an intrinsic property of the hadron [10]. For example, one of the three light-cone Fock wavefunctions of a $J_z = +1/2$ lepton in QED perturbation theory is $\psi^{\uparrow}_{+\frac{1}{2}+1}(x, \vec{k}_\perp) = -\sqrt{2}\frac{(-k^1 + \mathrm{i}k^2)}{x(1-x)}\varphi$, where $\varphi = \varphi(x, \vec{k}_\perp) = \frac{e/\sqrt{1-x}}{M^2 - (\vec{k}_\perp^2 + m^2)/x - (\vec{k}_\perp^2 + \lambda^2)/(1-x)}$. The orbital angular momentum projection in this case is $\ell^z = -1$. The spin structure indicated by perturbative theory provides a template for the numerator structure of the light-cone wavefunctions even for composite systems. The structure of the electron's Fock state in perturbative QED shows that it is natural to have a negative contribution from relative orbital angular momentum which balances the S_z of its photon constituents. We can also expect a significant orbital contribution to the proton's J_z since gluons carry roughly half of the proton's momentum, thus providing insight into the "spin crisis" in QCD.

The fall-off the light-cone wavefunctions at large $k_\perp$ and $x \to 1$ is dictated by QCD perturbation theory since the state is far-off the light-cone energy shell. This leads to counting rule behavior for the quark and gluon distributions at $x \to 1$. Notice that $x \to 1$ corresponds to $k^z \to -\infty$ for any constituent with nonzero mass or transverse momentum.

The above discussion suggests that an approximate form for the hadron light-cone wavefunctions might be constructed through variational principles and by minimizing the expectation value of H_{LC}^{QCD}.

12. Structure Functions are Not Parton Distributions

Ever since the earliest days of the parton model, it has been assumed that the leading-twist structure functions $F_i(x, Q^2)$ measured in deep inelastic lepton scattering are determined by the *probability* distribution of quarks and gluons as determined by the light-cone wavefunctions of the target. For example, the quark distribution is

$$P_{q/N}(x_B, Q^2) = \sum_n \int^{k_{i\perp}^2 < Q^2} \left[\prod_i dx_i\, d^2k_{\perp i}\right] |\psi_n(x_i, k_{\perp i})|^2 \sum_{j=q} \delta(x_B - x_j). \tag{13}$$

The identification of structure functions with the square of light-cone wavefunctions is usually made in LC gauge $n \cdot A = A^+ = 0$, where the path-ordered exponential in the operator product for the forward virtual Compton amplitude apparently reduces to unity. Thus the deep inelastic lepton scattering cross section (DIS) appears to be fully determined by the probability distribution of partons in the target. However, Paul Hoyer, Nils Marchal, Stephane Peigne, Francesco Sannino, and I have recently shown that the leading-twist contribution to DIS is affected by diffractive rescattering of a quark in the target, a coherent effect which is not included in the light-cone wavefunctions, even in light-cone gauge. The distinction between structure functions and parton probabilities is already implied by the Glauber-Gribov picture of nuclear shadowing [127, 128, 129, 130]. In this framework shadowing arises from interference between complex rescattering amplitudes involving on-shell intermediate states, as in Fig. 2. In contrast, the wave function of a stable target is strictly real since it does not have on energy-shell configurations. A probabilistic interpretation of the DIS cross section is thus precluded.

It is well-known that in Feynman and other covariant gauges one has to evaluate the corrections to the “handbag" diagram due to the final state interactions of the struck quark (the line carrying momentum p_1 in Fig. 2) with the gauge field of the target. In light-cone gauge, this effect also involves rescattering of a spectator quark, the p_2 line in Fig. 2. The light-cone gauge is singular – in particular, the gluon propagator $d^{\mu\nu}_{LC}(k) = \frac{i}{k^2+i\varepsilon}\left[-g^{\mu\nu} + \frac{n^\mu k^\nu + k^\mu n^\nu}{n\cdot k}\right]$ has a pole at $k^+ = 0$ which requires an analytic prescription. In final-state scattering involving on-shell intermediate states, the exchanged momentum k^+ is of $O(1/\nu)$ in the target rest frame, which enhances the second term in the propagator. This enhancement allows rescattering to contribute at leading twist even in LC gauge.

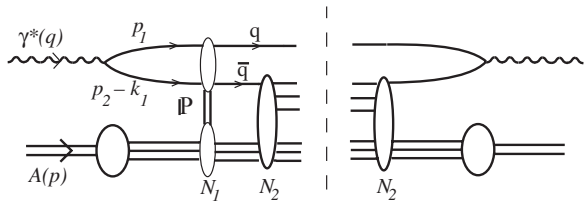

Figure 2: Glauber-Gribov shadowing involves interference between rescattering amplitudes.

The issues involving final state interactions even occur in the simple framework of abelian gauge theory with scalar quarks. Consider a frame with $q^+ < 0$. We can then distinguish FSI from ISI using LC time-ordered perturbation theory [5]. Figure 3 illustrates two LCPTH diagrams which contribute to the forward $\gamma^* T \to \gamma^* T$ amplitude, where the target T is taken to be a single quark. In the aligned jet kinematics the virtual photon fluctuates into a $q\bar{q}$ pair with limited transverse momentum, and the (struck) quark takes nearly all the longitudinal momentum of the photon. The initial q and $\bar{q}$ momenta are denoted p_1 and $p_2 - k_1$, respectively,

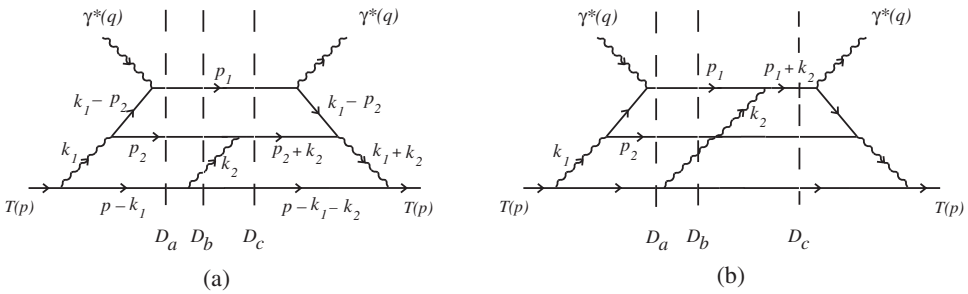

Figure 3: Two types of final state interactions. (a) Scattering of the antiquark (p_2 line), which in the aligned jet kinematics is part of the target dynamics. (b) Scattering of the current quark (p_1 line). For each LC time-ordered diagram, the potentially on-shell intermediate states – corresponding to the zeroes of the denominators D_a, D_b, D_c – are denoted by dashed lines.

The calculation of the rescattering effect of DIS in Feynman and light-cone gauge through three loops is given in detail in Ref. [131]. The result can be resummed and is most easily expressed in eikonal form in terms of transverse distances $r_\perp, R_\perp$ conjugate to $p_{2\perp}, k_\perp$. The deep inelastic cross section can be expressed as

$$Q^4 \frac{d\sigma}{dQ^2\, dx_B} = \frac{\alpha}{16\pi^2}\frac{1-y}{y^2}\frac{1}{2M\nu}\int \frac{dp_2^-}{p_2^-}\, d^2\vec{r}_\perp\, d^2\vec{R}_\perp\, |\widetilde{M}|^2 \tag{14}$$

where

$$|\widetilde{M}(p_2^-, \vec{r}_\perp, \vec{R}_\perp)| = \left| \frac{\sin\left[g^2 W(\vec{r}_\perp, \vec{R}_\perp)/2\right]}{g^2 W(\vec{r}_\perp, \vec{R}_\perp)/2} \widetilde{A}(p_2^-, \vec{r}_\perp, \vec{R}_\perp) \right| \tag{15}$$

is the resummed result. The Born amplitude is

$$\widetilde{A}(p_2^-, \vec{r}_\perp, \vec{R}_\perp) = 2eg^2 MQ p_2^- V(m_{||} r_\perp) W(\vec{r}_\perp, \vec{R}_\perp) \tag{16}$$

where $m_{||}^2 = p_2^- M x_B + m^2$ and

$$V(m\,r_\perp) \equiv \int \frac{d^2\vec{p}_\perp}{(2\pi)^2} \frac{e^{i\vec{r}_\perp\cdot\vec{p}_\perp}}{p_\perp^2 + m^2} = \frac{1}{2\pi} K_0(m\,r_\perp) \tag{17}$$

The rescattering effect of the dipole of the $q\overline{q}$ is controlled by

$$W(\vec{r}_\perp, \vec{R}_\perp) \equiv \int \frac{d^2\vec{k}_\perp}{(2\pi)^2} \frac{1 - e^{i\vec{r}_\perp\cdot\vec{k}_\perp}}{k_\perp^2} e^{i\vec{R}_\perp\cdot\vec{k}_\perp} = \frac{1}{2\pi} \log\left(\frac{|\vec{R}_\perp + \vec{r}_\perp|}{R_\perp}\right). \tag{18}$$

The fact that the coefficient of $\widetilde{A}$ in (15) is less than unity for all $\vec{r}_\perp, \vec{R}_\perp$ shows that the rescattering corrections reduce the cross section. It is the analog of nuclear shadowing in our model.

We have also found the same result for the deep inelastic cross sections in light-cone gauge. Three prescriptions for defining the propagator pole at $k^+ = 0$ have been used in the literature:

$$\frac{1}{k_i^+} \to \left[\frac{1}{k_i^+}\right]_{\eta_i} = \begin{cases} k_i^+ \left[(k_i^+ - i\eta_i)(k_i^+ + i\eta_i)\right]^{-1} & \text{(PV)} \\ \left[k_i^+ - i\eta_i\right]^{-1} & \text{(K)} \\ \left[k_i^+ - i\eta_i \varepsilon(k_i^-)\right]^{-1} & \text{(ML)} \end{cases} \tag{19}$$

the principal-value, Kovchegov [132], and Mandelstam-Leibbrandt [133] prescriptions. The 'sign function' is denoted $\varepsilon(x) = \Theta(x) - \Theta(-x)$. With the PV prescription we have $I_\eta = \int dk_2^+ \left[\frac{1}{k_2^+}\right]_{\eta_2} = 0$. Since an individual diagram may contain pole terms $\sim 1/k_i^+$, its value can depend on the prescription used for light-cone gauge. However, the $k_i^+ = 0$ poles cancel when all diagrams are added; the net is thus prescription-independent, and it agrees with the Feynman gauge result. It is interesting to note that the diagrams involving rescattering of the struck quark p_1 do not contribute to the leading-twist structure functions if we use the Kovchegov prescription to define the light-cone gauge. In other prescriptions for light-cone gauge the rescattering of the struck quark line p_1 leads to an infrared divergent phase factor $\exp i\phi$:

$$\phi = g^2 \frac{I_\eta - 1}{4\pi} K_0(\lambda R_\perp) + O(g^6) \tag{20}$$

where λ is an infrared regulator, and $I_\eta = 1$ in the K prescription. The phase is exactly compensated by an equal and opposite phase from final-state interactions of line p_2. This irrelevant change of phase can be understood by the fact that the different prescriptions are related by a residual gauge transformation proportional to $\delta(k^+)$ which leaves the light-cone gauge $A^+ = 0$ condition unaffected.

Diffractive contributions which leave the target intact thus contribute at leading twist to deep inelastic scattering. These contributions do not resolve the quark structure of the target, and thus they are contributions to structure functions which are not parton probabilities. More generally, the rescattering contributions shadow and modify the observed inelastic contributions to DIS.

The structure functions measured in deep inelastic lepton scattering are affected by final-state rescattering, thus modifying their connection with the light-cone probability distributions. In particular, the shadowing of nuclear structure functions is due to destructive interference effects from leading-twist diffraction of the virtual photon, physics not included in the nuclear light-cone wavefunctions.

Our analysis in the K prescription for light-cone gauge resembles the "covariant parton model" of Landshoff, Polkinghorne and Short [48, 134] when interpreted in the target rest frame. In this description of small x DIS, the virtual photon with positive q^+ first splits into the pair p_1 and p_2. The aligned quark p_1 has no final state interactions. However, the antiquark line p_2 can interact in the target with an effective energy $\hat{s} \propto k_\perp^2/x$ while staying close to its mass shell. Thus at small x and large $\hat{s}$, the antiquark p_2 line can first multiple scatter in the target via pomeron and Reggeon exchange, and then it can finally scatter inelastically or be annihilated. The DIS cross section can thus be written as an integral of the $\sigma_{\overline{q}p\to X}$ cross section over the p_2 virtuality. In this way, the shadowing of the antiquark in the nucleus $\sigma_{\overline{q}A\to X}$ cross section yields the nuclear shadowing of DIS [129]. Our analysis, when interpreted in frames with $q^+ > 0$, also supports the color dipole description of deep inelastic lepton scattering at small x. Even in the case of the aligned jet

configurations, one can understand DIS as due to the coherent color gauge interactions of the incoming quark-pair state of the photon interacting first coherently and finally incoherently in the target.

13. Acknowledgments

Work supported by the Department of Energy under contract number DE-AC03-76SF00515. Much of the new work reported here was done in collaboration with others, including Susan Gardner, John Hiller, Dae Sung Hwang, Paul Hoyer, Nils Marchal, Gary McCartor, Stephane Peigne, Francesco Sannino, and Prem Srivastava.

References

[1] D. Ashery [E791 Collaboration], hep-ex/9910024.
[2] G. Bertsch, S. J. Brodsky, A. S. Goldhaber and J. F. Gunion, Phys. Rev. Lett. **47**, 297 (1981).
[3] L. Frankfurt, G. A. Miller and M. Strikman, Phys. Lett. **B304**, 1 (1993) [hep-ph/9305228].
[4] L. Frankfurt, G. A. Miller and M. Strikman, Found. Phys. **30**, 533 (2000) [hep-ph/9907214].
[5] G. P. Lepage and S. J. Brodsky, Phys. Rev. D **22**, 2157 (1980).
[6] M. Beneke, G. Buchalla, M. Neubert and C. T. Sachrajda, Phys. Rev. Lett. **83**, 1914 (1999) [hep-ph/9905312].
[7] Y. Keum, H. Li and A. I. Sanda, hep-ph/0004004.
[8] S. J. Brodsky, H. Pauli and S. S. Pinsky, Phys. Rept. **301**, 299 (1998) [hep-ph/9705477].
[9] S. J. Brodsky and G. P. Lepage, in *Perturbative Quantum Chromodynamics*, A. H. Mueller, Ed. (World Scientific, 1989).
[10] S. J. Brodsky, D. S. Hwang, B. Ma and I. Schmidt, Nucl. Phys. **B593**, 311 (2001) [hep-th/0003082].
[11] P. P. Srivastava and S. J. Brodsky, Phys. Rev. D **64**, 045006 (2001) [arXiv:hep-ph/0011372].
[12] S. D. Drell and T. Yan, Phys. Rev. Lett. **24**, 181 (1970).
[13] G. B. West, Phys. Rev. Lett. **24**, 1206 (1970).
[14] S. J. Brodsky and S. D. Drell, Phys. Rev. D **22**, 2236 (1980).
[15] S. J. Brodsky and D. S. Hwang, Nucl. Phys. **B543**, 239 (1999) [hep-ph/9806358].
[16] S. J. Brodsky, M. Diehl and D. S. Hwang, Nucl. Phys. B **596**, 99 (2001) [arXiv:hep-ph/0009254].
[17] M. Diehl, T. Feldmann, R. Jakob and P. Kroll, Nucl. Phys. B **596**, 33 (2001) [Erratum-ibid. B **605**, 647 (2001)] [arXiv:hep-ph/0009255].
[18] S. J. Brodsky, M. Burkardt and I. Schmidt, distributions," Nucl. Phys. **B441**, 197 (1995) [hep-ph/9401328].
[19] S. J. Brodsky, hep-ph/0006310.
[20] S. J. Brodsky, P. Hoyer, C. Peterson and N. Sakai, Phys. Lett. **B93**, 451 (1980).
[21] B. W. Harris, J. Smith and R. Vogt, Nucl. Phys. **B461**, 181 (1996) [hep-ph/9508403].
[22] F. Antonuccio, S. J. Brodsky and S. Dalley, Phys. Lett. **B412**, 104 (1997) [hep-ph/9705413].
[23] S. J. Brodsky and A. H. Mueller, Phys. Lett. **B206**, 685 (1988).
[24] L. L. Frankfurt and M. I. Strikman, Phys. Rept. **160**, 235 (1988).
[25] S. J. Brodsky and B. T. Chertok, Phys. Rev. D **14**, 3003 (1976).
[26] S. J. Brodsky, C. Ji and G. P. Lepage, Phys. Rev. Lett. **51**, 83 (1983).
[27] G. R. Farrar, K. Huleihel and H. Zhang, Phys. Rev. Lett. **74**, 650 (1995).
[28] S. J. Brodsky, E. Chudakov, P. Hoyer and J. M. Laget, hep-ph/0010343.
[29] S. J. Brodsky, R. Roskies and R. Suaya, Momentum Frame," Phys. Rev. D **8**, 4574 (1973).
[30] J. M. Cornwall and J. Papavassiliou, Phys. Rev. D **40**, 3474 (1989).
[31] S. J. Brodsky and J. Rathsman, hep-ph/9906339.
[32] S. J. Brodsky, Y. Frishman, G. P. Lepage and C. Sachrajda, *Phys. Lett.* **91B**, 239 (1980).
[33] D. Müller, *Phys. Rev.* **D49**, 2525 (1994).
[34] V. M. Braun, S. E. Derkachov, G. P. Korchemsky and A. N. Manashov, Nucl. Phys. **B553**, 355 (1999), hep-ph/9902375.
[35] S. J. Brodsky and H. J. Lu, *Phys. Rev.* **D51**, 3652 (1995), hep-ph/9405218.
[36] S. J. Brodsky, J. R. Pelaez and N. Toumbas, Phys. Rev. **D60**, 037501 (1999), hep-ph/9810424.
[37] S. J. Brodsky, G. T. Gabadadze, A. L. Kataev and H. J. Lu, *Phys. Lett.* **B372**, 133 (1996) hep-ph/9512367.
[38] S. J. Brodsky, E. Gardi, G. Grunberg and J. Rathsman, Phys. Rev. D **63**, 094017 (2001) [arXiv:hep-ph/0002065].
[39] S. J. Brodsky, M. S. Gill, M. Melles and J. Rathsman, Phys. Rev. D **58**, 116006 (1998) [hep-ph/9801330].

[40] S. J. Brodsky and P. Huet, Phys. Lett. **B417**, 145 (1998), hep-ph/9707543.
[41] S. Chang, R. G. Root and T. Yan, Phys. Rev. D **7**, 1133 (1973).
[42] M. Burkardt, Nucl. Phys. **A504**, 762 (1989).
[43] H.-M. Choi and C.-R. Ji, Phys. Rev. **D 58**, 071901 (1998).
[44] K. Hornbostel, S. J. Brodsky and H. C. Pauli, Phys. Rev. D **41**, 3814 (1990).
[45] F. Antonuccio and S. Dalley, Phys. Lett. **B348**, 55 (1995) [hep-th/9411204].
[46] S. J. Brodsky, F. E. Close and J. F. Gunion, Phys. Rev. D **5**, 1384 (1972).
[47] S. J. Brodsky, F. E. Close and J. F. Gunion, Phys. Rev. D **6**, 177 (1972).
[48] S. J. Brodsky, F. E. Close and J. F. Gunion, Phys. Rev. D **8**, 3678 (1973).
[49] M. Diehl, T. Gousset and B. Pire, Phys. Rev. D **62**, 073014 (2000) [hep-ph/0003233].
[50] X. Ji, hep-ph/9610369.
[51] X. Ji, Phys. Rev. Lett. **78**, 610 (1997), hep-ph/9603249.
[52] A. V. Radyushkin, Phys. Lett. **B380**, 417 (1996) [hep-ph/9604317].
[53] X. Ji and J. Osborne, Phys. Rev. D **58**, 094018 (1998) [hep-ph/9801260].
[54] P. A. Guichon and M. Vanderhaeghen, Prog. Part. Nucl. Phys. **41**, 125 (1998) [hep-ph/9806305].
[55] M. Vanderhaeghen, P. A. Guichon and M. Guidal, Phys. Rev. Lett. **80**, 5064 (1998).
[56] A. V. Radyushkin, Phys. Rev. D **59**, 014030 (1999) [hep-ph/9805342].
[57] J. C. Collins and A. Freund, Phys. Rev. D **59**, 074009 (1999) [hep-ph/9801262].
[58] M. Diehl, T. Feldmann, R. Jakob and P. Kroll, Phys. Lett. **B460**, 204 (1999) [hep-ph/9903268].
[59] M. Diehl, T. Feldmann, R. Jakob and P. Kroll, Eur. Phys. J. **C8**, 409 (1999) [hep-ph/9811253].
[60] J. Blumlein and D. Robaschik, Nucl. Phys. **B581**, 449 (2000) [hep-ph/0002071].
[61] M. Penttinen, M. V. Polyakov, A. G. Shuvaev and M. Strikman, Phys. Lett. **B491**, 96 (2000) [hep-ph/0006321].
[62] S. J. Brodsky, SLAC-PUB-8649.
[63] G. P. Lepage and S. J. Brodsky, Phys. Lett. **B 87**, 359 (1979).
[64] S. D. Bass, S. J. Brodsky and I. Schmidt, Phys. Rev. D **60**, 034010 (1999) [hep-ph/9901244].
[65] S. J. Brodsky and G. R. Farrar, Phys. Rev. D **11**, 1309 (1975).
[66] G. P. Lepage and S. J. Brodsky, Phys. Rev. Lett. **43**, 545 (1979).
[67] A. Szczepaniak, E. M. Henley and S. J. Brodsky, Phys. Lett. **B243**, 287 (1990).
[68] A. Szczepaniak, Phys. Rev. D **54**, 1167 (1996).
[69] Y. Y. Keum, H. Li and A. I. Sanda, hep-ph/0004173.
[70] H. Li, hep-ph/0012140.
[71] S. J. Brodsky and G. P. Lepage, Phys. Rev. D **24**, 2848 (1981).
[72] S. J. Brodsky, C. Ji, A. Pang and D. G. Robertson, Phys. Rev. D **57**, 245 (1998) [hep-ph/9705221].
[73] S. J. Brodsky and G. P. Lepage, in *C81-04-06.1.4* Phys. Rev. D **24**, 1808 (1981).
[74] E. Braaten and S. Tse, Phys. Rev. D **35**, 2255 (1987).
[75] J. Gronberg *et al.* [CLEO Collaboration], Phys. Rev. **D57**, 33 (1998), hep-ex/9707031; and H. Paar, presented at PHOTON 2000: International Workshop on Structure and Interactions of the Photon Ambleside, Lake District, England, 26-31 Aug 2000.
[76] A. V. Radyushkin, Acta Phys. Polon. **B26**, 2067 (1995) [hep-ph/9511272].
[77] S. Ong, Phys. Rev. D **52**, 3111 (1995).
[78] P. Kroll and M. Raulfs, Phys. Lett. **B387**, 848 (1996) [hep-ph/9605264].
[79] V. L. Chernyak and A. R. Zhitnitsky, Phys. Rept. **112**, 173 (1984).
[80] D. Muller, D. Robaschik, B. Geyer, F. M. Dittes and J. Horejsi, Fortsch. Phys. **42**, 101 (1994) [hep-ph/9812448].
[81] Paar, H., *et al.* CLEO collaboration (to be published); See also Boyer, J. *et al.*, *Phys. Rev. Lett.* **56**, 207 (1980); TPC/Two Gamma Collaboration (H. Aihara *et al.*), *Phys. Rev. Lett.* **57**,404 (1986).
[82] G. R. Farrar and H. Zhang, Phys. Rev. Lett. **65**, 1721 (1990).
[83] T. C. Brooks and L. Dixon, Phys. Rev. D **62**, 114021 (2000) [hep-ph/0004143].
[84] H. M. Sommermann, R. Seki, S. Larson and S. E. Koonin, Phys. Rev. D **45**, 4303 (1992).
[85] S. Brodsky and M. Karliner, in preparation.
[86] S. J. Brodsky, V. S. Fadin, V. T. Kim, L. N. Lipatov and G. B. Pivovarov, JETP Lett. **70**, 155 (1999) [hep-ph/9901229].
[87] A. Donnachie and P. V. Landshoff, hep-ph/0105088.
[88] S. J. Brodsky and D.-S. Hwang, in preparation.

[89] S. Brodsky, M. Diehl, P. Hoyer, and S. Peigne, in preparation.
[90] L. Frankfurt, G. A. Miller and M. Strikman, hep-ph/0010297.
[91] E. M. Aitala *et al.* [E791 Collaboration], Phys. Rev. Lett. **86**, 4773 (2001) [hep-ex/0010044].
[92] E. M. Aitala *et al.* [E791 Collaboration], Phys. Rev. Lett. **86**, 4768 (2001) [hep-ex/0010043].
[93] V. M. Braun, D. Y. Ivanov, A. Schafer and L. Szymanowski, *Phys. Lett. B* **509**, 43 (2001) [hep-ph/0103275].
[94] V. Chernyak, [hep-ph/0103295].
[95] G. A. Miller, S. J. Brodsky and M. Karliner, Phys. Lett. **B481**, 245 (2000) [hep-ph/0002156].
[96] G. A. Miller, Int. J. Mod. Phys. B **15**, 1551 (2001) [nucl-th/9910053].
[97] M. Franz, M. V. Polyakov and K. Goeke, Phys. Rev. D **62**, 074024 (2000) [hep-ph/0002240].
[98] S. J. Brodsky and M. Karliner, Phys. Rev. Lett. **78**, 4682 (1997) [hep-ph/9704379].
[99] C. V. Chang and W. Hou, in *B* Meson," hep-ph/0101162.
[100] S. J. Brodsky and F. S. Navarra, Phys. Lett. B **411**, 152 (1997) [hep-ph/9704348].
[101] S. J. Brodsky and S. Gardner, hep-ph/0108121.
[102] M. Ciuchini, E. Franco, G. Martinelli, M. Pierini and L. Silvestrini, Phys. Lett. B **515**, 33 (2001) [hep-ph/0104126].
[103] H. C. Pauli and S. J. Brodsky, Phys. Rev. D **32**, 2001 (1985).
[104] S. Dalley and I. R. Klebanov, Phys. Rev. D **47**, 2517 (1993) [hep-th/9209049].
[105] F. Antonuccio and S. Dalley, Phys. Lett. **B376**, 154 (1996) [hep-th/9512106].
[106] F. Antonuccio and S. Dalley, Nucl. Phys. **B461**, 275 (1996) [hep-ph/9506456].
[107] S. J. Brodsky, J. R. Hiller and G. McCartor, Phys. Rev. D **58**, 025005 (1998) [hep-th/9802120].
[108] S. J. Brodsky, J. R. Hiller and G. McCartor, Phys. Rev. D **60**, 054506 (1999) [hep-ph/9903388].
[109] S. Dalley and B. van de Sande, Phys. Rev. D **62**, 014507 (2000) [hep-lat/9911035].
[110] J. R. Hiller and S. J. Brodsky, Phys. Rev. D **59**, 016006 (1999) [hep-ph/9806541].
[111] F. Antonuccio, I. Filippov, P. Haney, O. Lunin, S. Pinsky, U. Trittmann and J. Hiller [SDLCQ Collaboration], hep-th/9910012. Brodsky:1999xj
[112] O. Lunin and S. Pinsky, hep-th/9910222.
[113] P. Haney, J. R. Hiller, O. Lunin, S. Pinsky and U. Trittmann, Phys. Rev. D **62**, 075002 (2000) [hep-th/9911243].
[114] G. P. Lepage, S. J. Brodsky, T. Huang and P. B. Mackenzie, CLNS-82/522, published in Banff Summer Inst.1981:0083 (QCD161:B23:1981); S. J. Brodsky, T. Huang and G. P. Lepage, *In *Banff 1981, Proceedings, Particles and Fields 2*, 143-199*.
[115] D. Daniel, R. Gupta and D. G. Richards, Phys. Rev. D **43**, 3715 (1991).
[116] L. Del Debbio, M. Di Pierro, A. Dougall and C. Sachrajda [UKQCD collaboration], Nucl. Phys. Proc. Suppl. **83**, 235 (2000) [hep-lat/9909147].
[117] G. Martinelli and C. T. Sachrajda, Amplitude," Phys. Lett. **B190**, 151 (1987).
[118] S. Dalley, hep-ph/0007081.
[119] W. A. Bardeen and R. B. Pearson, Phys. Rev. D **14**, 547 (1976).
[120] M. Burkardt, Phys. Rev. D **54**, 2913 (1996) [hep-ph/9601289].
[121] V. Y. Petrov, M. V. Polyakov, R. Ruskov, C. Weiss and K. Goeke, Phys. Rev. D **59**, 114018 (1999) [hep-ph/9807229].
[122] D. Diakonov and V. Y. Petrov, hep-ph/0009006.
[123] M. B. Hecht, C. D. Roberts and S. M. Schmidt, nucl-th/0008049.
[124] P. P. Srivastava and S. J. Brodsky, Phys. Rev. **D61**, 025013 (2000), hep-ph/9906423, and SLAC-PUB 8543, in preparation.
[125] H. C. Pauli and S. J. Brodsky, Phys. Rev. D **32**, 1993 (1985).
[126] S. J. Brodsky, J. R. Hiller and G. McCartor, hep-ph/0107038.
[127] V. N. Gribov, Sov. Phys. JETP **29**, 483 (1969) [Zh. Eksp. Teor. Fiz. **56**, 892 (1969)].
[128] S. J. Brodsky and J. Pumplin, Phys. Rev. **182**, 1794 (1969).
[129] S. J. Brodsky and H. J. Lu, Phys. Rev. Lett. **64**, 1342 (1990).
[130] G. Piller and W. Weise, Phys. Rept. **330**, 1 (2000) [hep-ph/9908230].
[131] S. J. Brodsky, P. Hoyer, N. Marchal, S. Peigne and F. Sannino, hep-ph/0104291.
[132] Y. V. Kovchegov, Phys. Rev. D **55**, 5445 (1997) [hep-ph/9701229].
[133] G. Leibbrandt, Rev. Mod. Phys. **59**, 1067 (1987).
[134] P. V. Landshoff, J. C. Polkinghorne and R. D. Short, Nucl. Phys. B **28**, 225 (1971).